Identification of pH-sensitive regions in the mouse prion by the cysteine-scanning spin-labeling ESR technique

Yasuko Watanabe[a], Osamu Inanami[a], Motohiro Horiuchi[b], Wakako Hiraoka[c], Yuhei Shimoyama[d], Fuyuhiko Inagaki[e] and Mikinori Kuwabara[a]

[a]Laboratory of Radiation Biology and [b]Prion Disease, Graduate School of Veterinary Medicine, Hokkaido University, Sapporo 060-0818, Japan

[c]Laboratory of Biophysics, School of Science and Technology, Meiji University, Kawasaki 214-8571, Japan

[d]Soft-Matter Physics Laboratory, Graduate School of Emergent Science, Muroran Institute of Technology, Muroran 050-8585, Japan

[e]Laboratory of Structural Biology, Graduate School of Veterinary Medicine, Hokkaido University, Sapporo 060-0818, Japan

Corresponding author: Osamu Inanami, Ph.D.

Laboratory of Radiation Biology, Department of Environmental Veterinary Sciences, Graduate School of Veterinary Medicine, Hokkaido University, Kita 18-Jo Nishi 9-chome, Sapporo 060-0818, JAPAN

Tel: +81-11-706-5236

Fax: +81-11-706-7373

E-mail: inanami@vetmed.hokudai.ac.jp

Abstract

We analyzed the pH-induced mobility changes in moPrP^{C} α-helix and β-sheets by cysteine-scanning site-directed spin labeling (SDSL) with ESR. Nine amino acid residues of α-helix1 (H1, codon143-151), four amino acid residues of β-sheet1 (S1, codon127-130) and four amino acid residues of β-sheet2 (S2, codon160-163) were substituted for by cysteine residues. These recombinant mouse PrP^{C} (moPrP^{C}) mutants were reacted with a methane thiosulfonate sulfhydryl-specific spin labeling reagent (MTSSL). The 1/δH of the central (^{14}N hyperfine) component (M_I=0) in the ESR spectrum of spin-labeled moPrP^{C} was measured as a mobility parameter of nitroxide residues (R1). The mobilities of E145R1 and Y149R1 at pH 7.4, which was identified as a tertiary contact site by a previous NMR study of moPrP, were lower than those of D143R1, R147R1 and R150R1 reported on the helix surface. Thus, the mobility in the H1 region in the neutral solution was observed with the periodicity associated with a helical structure. On the other hand, the values in the S2 region, known to be located in the buried side, were lower than those in the S1 region located in the surface side. These results indicated that the mobility parameter of the nitroxide label was well correlated with the 3D structure of moPrP. Furthermore, the present study clearly demonstrated three pH-sensitive sites in moPrP, *i.e.*, (1) the N-terminal tertiary contact site of H1, (2) the C-terminal end of H1 and (3) the S2 region. In particular, among these pH-sensitive sites, the N-terminal tertiary contact region of H1 was found to be the most pH-sensitive one and was easily converted to a flexible structure by a slight decrease of pH in the solution. These data provided molecular evidence to explain the cellular mechanism for conversion from PrP^{C} to PrP^{Sc} in acidic organelles such as the endosome.

Key words: SDSL; ESR; prion; domain mobility; pH-sensitive region

Introduction

Transmissible spongiform encephalopathies (TSEs), or prion diseases, are a group of fatal neurodegenerative disorders including Creutzfeldt-Jacob disease, Gerstmann-Sträusler-Scheinker syndrome, fatal familial insomnia and kuru in humans, scrapie in sheep and bovine spongiform encephalopathy (BSE) in cattle [1, 2]. According to the "prion-only hypothesis" [1, 3, 4], the abnormal (scrapie-like and β-sheet-rich) form of prion protein (PrP^{Sc}) converted from the normal cellular prion protein (PrP^{C}) is recognized as the only pathogenic component of TSEs. Mammalian PrP^{C} is a ubiquitous glycoprotein attached to the plasma membrane via a glycosyl phosphatidylinositol (GPI) anchor [1]. As illustrated in Figure 1A, mouse PrP (moPrP) consists of 208 amino acids (residues 23-231). The carboxy-terminal domain of moPrP (121-231) is defined as a tertiary structure and contains three α-helices (Helix1, Helix2 and Helix3) and two short anti-parallel β-sheets (Sheet1 and Sheet2) [1, 5, 6].

Though the precise mechanism of conversion from PrP^{C} to PrP^{Sc} is still unknown, the accumulation of PrP^{Sc} in endosomes, the main intracellular acidic organelles, indicates that the process of conversion from PrP^{C} to PrP^{Sc} requires physiological acidic pH conditions [7-9]. Recent circular dichroism (CD) spectroscopic studies showed that acidic conditions in the presence of a denatured agent induce a β-sheet-rich intermediate in human (90-231) and mouse PrP (121-231) *in vitro* [7, 10, 11]. The study, which used antibodies to probe the structure of recombinant Sylian hamster PrP (residues 90-231), indicated that the conformation of epitopes localized in the C-terminus was insensitive to pH, whereas that of the N-terminus was sensitive [12]. NMR measurement of the full-length human PrP showed that the octapeptide repeats in the N-terminal domain constituted pH-dependent PrP oligomerization; however, this was not detectable around pH-sensitive regions in the C-terminal domain [13]. In contrast, studies using molecular dynamics (MD) simulations

proposed the presence of a pH-sensitive region in the C-terminal globular domain on Sylian hamster PrP 109-219, human PrP 125-228 and bovine PrP 124-227 [14, 15]. In fact, high resolution NMR and the thermal stability of the globular domain of truncated prion protein (hPrP 121-230) suggested that the residues at the C-terminal end of helix1 and residues 161-164 of β-strand2 were candidates for the "starting point" of pH-induced unfolding and implicated in endosomic PrP^{C} to PrP^{Sc} conformational transition resulting in TSEs [16]. However, for the full-length PrP^{C}, there is no experimental evidence that low pH induces a conformational change in the globular region of PrP.

Recently, site-directed spin labeling (SDSL) combined with electron spin resonance spectroscopy (ESR) has proven to be a useful technique for protein structural and motional analyzes, such as determination of the secondary structure and its orientation, areas of tertiary interactions and domain mobility [17-20]. The data of SDSL-ESR are applicable for conformational analysis of high molecular weight proteins, whereas NMR and X-ray crystallographic methods are impossible to use for such analysis [17]. In SDSL, the nitroxide side chain (R1) derived from a sulfhydryl-specific nitroxide agent such as a methane thiosulfonate spin label (MTSSL) is introduced into the target codon in the protein sequences by using site-directed mutagenesis (Fig. 1B). Recently, by using this cysteine-scanning spin labeling method to obtain structual information on erythroid α and β spectrin peptides, which are not easily studied by either NMR or X-ray methods, a new amphipathic nature of the helical regions, which is critical in αβ spectrin association at the tetramerization site, was reported by Mehboob *et al.* [21], indicating that this technique is a powerful tool for monitoring the structure and dynamics of proteins. We have also applied this method to obtain biophysical information on moPrP and reported the thermal stability and pH-dependent mobility changes in three recombinant moPrP mutations (N96C, D143C and T189C) labeled with MTSSL on the full-length prion protein [22].

In the present study, we used the cysteine-scanning spin-labeling method to analyze the dynamics of recombinant moPrP mutants that were singly labeled at seventeen residues in α-helix1 (H1, codon143-151), β-sheet1 (S1, codon127-130) and β-sheet2 (S2, codon160-163). We determined the locations of the pH-sensitive protein sequences in the H1 and S2 regions.

Materials and Methods

Materials. (1-Oxy-2,2,5,5-tetramethyl-3-pyrroline-3-methl)methanethiosulfonate (MTSSL) was purchased from Toronto Research Chemicals (ON, Canada). *E. coli* BL21(DE3)LysS and isopropylthio-β-$_D$-galactoside (IPTG) were from Invitrogen (CA, USA). Ni Sepharose 6 Fast Flow was from Amersham Biosciences Co. (NJ, USA). The TSKgel Phenyl-5PW RP column was from TOSOH (Tokyo, Japan). The Protein Assay Lowry Kit was from Nacalai Tesque, Inc. (Kyoto, Japan). 2-[4-(2-Hydroxyethyl)-1-piperazinyl]ethanesulfonic acid (HEPES) and 2-morpholinoethanesulfonic acid, monohydrate (MES) were from Dojindo, Lab. (Kumamoto, Japan). Other reagents were from Wako Pure Chemical, Co. (Tokyo, Japan).

Construction of moPrP mutants. cDNA encoding mouse PrP (residues 23-231) was cloned into BamHI/EcoRI sites of pRSETb as described previously [22, 23]. In the plasmid encoding moPrP, single amino acids at H1, S1 and S2 were substituted for by cysteine residues (Fig. 1A). These moPrP mutants were generated by the PCR-based site-directed mutagenesis method [22, 24]. Oligonucleotides used in the mutagenesis were obtained from Sigma Genosys. The change of the target codons by cysteine residues was confirmed using a CEQ8800 automated sequencer (Beckman Coulter, Inc.).

Expression and Purification of recombinant moPrP mutants. The expression and purification of recombinant moPrP mutants were modified from those described previously [22]. The expression plasmids were introduced into *E. coli* BL21(DE3)LysS. *E. coli* BL21(DE3)LysS with each moPrP construct was grown overnight in 100 ml of SOB liquid culture medium containing 1% sucrose and 0.1 mg/ml ampicillin and 0.05 mg/ml chloramphenicol at 37°C. Then 15 ml of overnight culture was added to 450 ml of SOB medium with 1% sucrose and 0.1 mg/ml ampicillin and 0.05 mg/ml chloramphenicol and grown at 37°C to an optical density at 600 nm of 0.7. Protein expression was induced by adding IPTG to a final concentration at 0.5 mM. The culture was continued for 7 h and then bacterial cells were collected by centrifugation. The bacterial pellets were suspended in 6 M GdnHCl in 20 mM Na_2HPO_4 (pH 7.8) and sonicated to completely release the inclusion bodies from BL21(DE3)LysS transformed with expression plasmids. Separated inclusion bodies in 6 M GdnHCl in 20 mM Na_2HPO_4 (pH 7.8) were incubated with Ni^{2+}-charged chelating sepharose for 1 h to purify the recombinant moPrP. The protein-bound sepharose was washed 2 times with 8 M urea in 10 mM Tris/HCl and 100 mM NaH_2PO_4 (pH 6.2) and then loaded into the column. The recombinant moPrP was eluted using 8 M urea in 10 mM Tris/HCl and 100 mM NaH_2PO_4 (pH 4.2). After dialysis against 10 mM acetate buffer (pH 4.0) for 48 h, recombinant moPrP was purified by reverse-phase high performance liquid chromatography (HPLC) using TSKgel Phenyl-5PW RP and a 40-60% linear gradient of acetonitrile with 0.05% trifluoroacetic acid. The purified recombinant moPrP was dialyzed against 10 mM acetate buffer (pH 4.0) for 48 h and concentrated with a centrifugal concentrator (Vivascience) to approximately a quarter of its original volume and then stored at -80°C until use. The protein concentration was quantified with the Lowry protein assay using BSA as a standard [25]. The final protein purity (>98%) was confirmed by sodium dodecyl sulfate polyacrylamide gel electrophoresis (SDS-PAGE) and Commasie Brilliant Blue staining.

Spin-labeling of moPrP mutants. To label the moPrP mutants with MTSSL, a 10-fold molar excess of MTSSL was added to each protein and incubated overnight in the dark at 4°C. The free MTSSL was removed from the protein using a microdialyzer (Nippon Genetics). To confirm that the α-helix content of spin-labeled moPrP mutants was similar to that of wild-type moPrP, we used a far-UV CD spectropolarimeter (J-820, JASCO) [22]. The sample was diluted to 0.3 mg/ml protein concentration and scanned using a scan speed of 50 nm/min and a response time of 2 sec. In all mutants, the two minima (208 and 220 nm), typical of a mainly α-helix-structure protein, were clearly observed and there were no differences in the α-helix content between wild-type moPrP and spin-labeled moPrP mutants [22, 26].

ESR spectroscopy. Details of the ESR spectroscopy methods have been published elsewhere [22]. The pH change of the sample solution was carried out by dialysis of the sample against the three buffers, 10 mM acetate buffer (pH 5.0), 10 mM MES buffer (pH 6.4) and 10 mM HEPES buffer (pH 7.4). ESR spectra were recorded in a quartz flat cell (RST-DVT05; 50 mm x 4.7 mm x 0.3 mm, Radical Research) for spin-labeled samples of 20 μM moPrP using a JEOL-RE X-band spectrometer (JEOL) with a cylindrical TE011 mode cavity (JEOL). All ESR spectra were obtained at 20°C, controlled by a temperature controller (ES-DVT4, JEOL), under the following conditions: 5 mW incident microwave power, 100 kHz modulation frequency, 0.2 mT field modulation amplitude and 10 mT scan range. The $1/\delta H_0$ of the central component (M_I=0: ^{14}N hyperfine) in the ESR spectrum of spin-labeled $moPrP^C$ was employed as a mobility parameter and was further analyzed using a Win-Rad Radical Analyzer System (Radical Research). To reveal the motional change upon pH variation, we further examined the second moment $\langle H^2 \rangle$, a measure of spectral deviation due to the motional narrowing (or broadening) of ESR spectra. The second moment was estimated

numerically with the Win-Rad System.

Results

Mobility change with pH: ESR spectral features from moPrP^C

Figure 2A shows the ESR spectra from recombinant full length moPrP mutants in the H1 region at pH 7.4 at 20^{o}C. Each ESR spectrum from the nine mutants in the H1 region of moPrP showed a different line shape (Fig. 2A). In general, the ESR spectra from H1 region indicate mobile signals with small immobile contributions. The ESR spectra obtained from E145R1 and Y149R1 showed line broadening as compared with those of D143R1 or R150R1, indicating the immobility of the nitroxide probe in E145R1 and Y149R1. To obtain detailed mobility information, we measured the inverse of the peak-to-peak first derivative width of the central resonance ($1/\delta H_0$) in each ESR spectrum in the H1 region, since it has been reported by Hubbell *et al.* that $1/\delta H_0$ from the ESR spectrum as a mobility parameter is strongly correlated with the local environment of the protein domain structure [17]. The values of $1/\delta H_0$ obtained from the ESR spectra of D143R1, R147R1, R150R1 and E151R1 were approximately 4.07, 2.82, 3.50 and 3.35, respectively. On the other hand, those obtained from the ESR spectra of E145R1 and Y149R1 were approximately 2.19 and 2.75, respectively. The plotted data of $1/\delta H_0$ shown in Fig. 2B indicate the periodical changes in the H1 region. In the S1 region, the ESR spectrum of M129R1 was slightly narrower than those of the other positions in S2 (Fig. 3A) and the $1/\delta H_0$ (3.20) of the M128R1 mutant was slightly higher than those of Y127R1 (2.86), L129R1 (2.88) and G130R1 (2.84) (Fig. 3B). In the S2 region, there were no differences in the line shapes of the ESR spectra of V160R1, Y161R1, Y162R1 and R163R1 (Fig. 4A) and the values of $1/\delta H_0$ from the ESR spectra of these four mutants ranged

from 2.1 to 2.3, indicating that the nitroxide probes in S2 were strongly immobilized in comparison with those in S1 (Fig. 4B).

pH-induced conformational changes in moPrP^{C}

Since it has been suggested that acidic pH is involved in the conformational transition from PrP^{C} to PrP^{Sc} [7-9], we examined the effects of pH changes on the line shapes of ESR spectra of moPrP^{C} as shown in Fig. 2A, 3A and 4A. In the H1 region, each mutant showed a different pattern for the variation of the ESR spectrum during the reduction of pH. When pH in the solution decreased from pH 7.4 to pH 5.0 at 20^{o}C, there was no significant change in the ESR spectrum of D143R1, but the ESR spectrum of E145R1 became narrow, indicating a pH-dependent conformational change from a rigid to a flexible structure. In contrast to this, the decrease of pH induced line broadening in the ESR spectra of R150R1 and R151R1. In the β-sheet regions, no pH-dependent changes in the line shapes of ESR spectra of S1 were observed (Fig. 3A). However, the decrease of pH induced narrow line shapes in the ESR spectra of V160R1 and Y161R1 in S2.

Figures 2B, 3B and 4B show the pH-dependent changes of $1/\delta H_0$ from ESR spectra in various regions at 20^{o}C. In the H1 region, the value of $1/\delta H_0$ of D143R1 at pH 5.0 was similar to that of pH 7.4. However the $1/\delta H_0$ of E145R1 increased from 2.2 to 2.5 when the pH in the solution slightly changed from 7.4 to 6.4, and remained constant at the high level of pH 5.0. The values of $1/\delta H_0$ of D146R1 and R147R1 also slightly increased at pH 6.4 in comparison with pH 7.4. In contrast, the values of $1/\delta H_0$ of R150R1 and E151R1 decreased when the pH in the solution decreased from 6.4 to 5.0. On the other hand, the pH-dependent change in $1/\delta H_0$ was not observed in the S1 region. The values of $1/\delta H_0$ of V160R1, Y161R1, Y162R1 and R163R1 in the S2 region increased when pH in the solution decreased from 6.4 to 5.0, but

the changes in $1/\delta H_0$ of Y162R1 and R163R1 resulting from a decrease of pH from 6.4 to 5.0 were relatively small.

Discussion

Structural studies by NMR of recombinant hPrP (23-230) [13, 27], moPrP (23-231) [28] and hamster PrP (29-231) [29] revealed a highly flexible N-terminal octapeptide repeat region and C-terminal global region. Figures 5B and 5C show global features of the refined NMR structure of the C-terminal globular region, mPrP (121-231) as reported by Rick et al. [30]. Prion proteins in the cell are attached to the plasma membrane via a glycosyl phosphatidylinositol (GPI) anchor and localized in membrane lipid rafts [1, 31]. Lipid rafts, which are rich in spingolipids and cholesterol, are associated with endocytosis. Endosomes and lysosomes are typical acidic organelles [32], their luminal pH is formed by vacuolar type proton ATPase (V-ATPase) and varies between 6.5 and 4.5 [33, 34]. Many past studies demonstrated the relationship between the pH of intracellular acidic compartments and conversion from PrP^C to PrP^{Sc} [7-16, 35]. Recently, the *in vivo* conversion of human brain PrP^C to a PrP^{Sc}-like form was reported to be enhanced at acidic pH [36] and biophysical studies have shown that the free energy of unfolding of hPrP(90-231) is lower at acidic pH than at neutral pH [10]. A β-sheet-rich folding intermediate was observed for moPrP (121-231) at low pH in urea but was also seen at neutral pH [37]. The mechanism for pH-dependent structural changes of prion protein were reported in molecular dynamics (MD) simulation studies [14, 15, 38]. On the other hand, experimental data about the pH-sensitive region of prion proteins seem to be insufficient although there was one report suggesting that the C-terminal end of Helix1 and 161-164 of S2 have a larger tendency to unfold as revealed by NMR with amide proton protection factor mapping of the globular domain of PrP [16].

The SDSL-ESR technique can be used to analyze high molecular weight proteins for which NMR spectroscopic and X-ray crystallographic methods are not generally applicable [17-20]. In the present study, we employed the SDSL-ESR technique to obtain experimental information on pH-sensitive regions of recombinant moPrP^{C}. Hubbell *et al.* first used the inverse of peak-to-peak first derivative width of the central resonance ($1/\delta H_0$) of the ESR spectrum as a mobility parameter [17]. We also measured the $1/\delta H_0$ in ESR spectra at pH 7.4 and 20^{o}C. Figures 2B, 3B and 4B show the values of $1/\delta H_0$ obtained from the cysteine-scanning SDSL-ESR data of H1, S1 and S2, respectively. In the H1 region, a periodical change of $1/\delta H_0$ was observed. In comparison with the 3D structure of moPrP as estimated by NMR data, shown in Fig. 5B, highly mobile residues of the nitroxide probe in D143R1, R147R1 and R150R1 were located on the outer surface of H1, whereas low mobility residues such as E145R1 and Y149R1 were in the inner contact residues of H1. These variations of mobility in the nitroxide probe were well-correlated with the 3D helix structure of moPrP. On the other hand, the fluctuation in the values of $1/\delta H_0$ of the S1 region in neutral pH solution of moPrP was small, although the value at M128R1 was observed to be relatively high (Fig. 3B). Furthermore, the values of $1/\delta H_0$ of the S2 region were lower than those of the S1 region (Figs. 3B and 4B). The 3D structure of moPrP identified by NMR (Fig. 5B) showed that the S2 region was located in the buried structure close to H2 and H3, whereas the S1 region was located in the relatively outer side of moPrP. The difference of mobility between S1 and S2 regions can probably be explained by the difference of the tertiary structure of moPrP. To define the relationship between structure and mobility, with the aide of $1/\delta H_0$, it is convenient to employ a further semiempirical parameter for mobility reflected in ESR spectra: namely the spectral breadth, which is represented by the spectral second moment ($<H^2>$) [39]. The numerical values of these quantities are mainly determined by the degree of averaging of

magnetic tensor values. As the frequency of nitroxide rotational motion is lowered, the second moment and the line width increase. Figure 5A shows a plot of the reciprocal second moment ($1/\langle H^2 \rangle$) versus the reciprocal central line width ($1/\delta H_0$) for the spectra of R1 side chains representing the helix surface, helix tertiary contact and two β-sheets (S1 and S2). As shown in Fig. 5A, the mobility was consistent with the tertiary fold of moPrP and there was a linear correlation between these two parameters. These results indicated that these parameters were related to the 3D structure of PrP.

Since recent reports [7-16, 35] showed that exposure of prion proteins to low pH in endosomes was essential for the conversion from PrP^C to PrP^{Sc}, we tried to identify pH-sensitive regions by using the cysteine-scanning spin-labeling technique as described above. In the H1 region, we observed increases of $1/\delta H_0$ at E145R1, D146R1 and R147R1 when pH was decreased from 7.4 to 6.4 (Fig. 2). The values of R150R1 and E151R1 at pH 6.4 were similar to those at pH 7.4, but these values suddenly dropped when the pH in the solution changed from pH 6.4 to pH 5.0 as shown in Fig. 2B. In β-sheet regions of PrP, as shown in Fig. 3B, the mobility of S1 was conserved against a decrease of pH. However, the values of $1/\delta H_0$ at all four residues of S2 increased when pH was decreased from 6.4 to 5.0 (Fig. 4B). In particular, the region containing two N-terminal residues of S2, V160R1 and Y161R1, was identified as a more pH-sensitive region than that of C-terminal side residues of S2. Thus, the pH-sensitive domains, including the N-terminal tertiary contact site of H1 and the C-terminal ends of H1 and S2 regions, were identified in recombinant moPrP as shown in Fig. 5C. It is noteworthy that a slight decrease from pH 7.4 to pH 6.4 induced conformational changes in the N-terminal tertiary contact residues of H1 (E145R1, D146R1 and R147R1) though conformational changes in the C-terminal end of H1 (R150R1 and E151R1) and N-terminal residues of S2 (160R1 and Y161R1) required a large change from pH 7.4 to pH 5.0. These findings led us to speculate that the conformational change from the tertiary

contact structure to a more flexible structure in N-terminal residues of H1 was the first step for unfolding of PrP, followed by secondary conformational changes of S2 and the C-terminal end of H1.

In a previous NMR study of the globular domain (121-231) of hPrP [16], two domains, the C-terminal ends of the H1 and S2 regions, were identified as the pH-sensitive regions for acid-induced unfolding leading to a β-sheet rich structure. In addition to these two sites, the present SDSL-ESR study clearly demonstrated that the N-terminal region (E145, D146 and R147) of H1 was also a pH-sensitive region. The N-terminal tertiary contact region of H1 may be important for conversion from PrP^{C} to PrP^{Sc} in acidic conditions, since the structural change in this region easily occurred in a mildly acidic condition (pH 6.4) in comparison with the other two pH-sensitive regions. According to recent studies using MD simulations for PrP, histidine at 186 and asparagic acid at 177 of PrP were reported to be candidates for the amino acid residues that trigger the conversion to β-sheet-rich PrP [38, 40]. This conversion model was based on the 3D structural changes due to disruption of a salt bridge with protonation of their amino acid residues caused by a decrease of pH. It is unclear whether these amino-acid residues were actually associated with pH-dependent conformational changes in H1 and S2 as observed in the present study. Further experiments to clarify this are now in progress.

In summary, the present cysteine-scanning SDSL-ESR study for H1, S1 and S2 of moPrP provided experimental evidence for three pH-sensitive sites, (1) the N-terminal tertiary contact site of H1, (2) the C-terminal end of H1 and (3) the S2 region. In particular, the present identification is the first report on a conformational change in the N-terminal tertiary contact site of H1 induced by mildly acidic conditions. This conformational change may be the first step in conversion of PrP^{C} to the pathogenic PrP^{Sc} structure in intracellular acidic organelles.

Acknowledgments

This work was supported, in part, by Grants-in-Aid for Basic Scientific Research from the Ministry of Education, Culture, Sports, Science and Technology of Japan (No. 17380178 and No. 18658118 [O.I.] and No. 17580275 and No. 17658126 [M.K.]), by Research Grants from the Program for the Center of Excellence of Zoonosis Control, Sapporo 060-0818, Japan [Y.W., O.I., M.H.] and CREST-JST, Multi-Quantum Coherence ESR Project, Muroran 050-8585, Japan [Y.S.].

References

[1] S.B. Prusiner, Prions, Proc. Natl. Acad. Sci. USA 95 (1998) 13363-13383.

[2] C. Weissmann, The Ninth Datta Lecture. Molecular biology of transmissible spongi form encephalopathies, FEBS Lett. 389 (1996) 3-11.

[3] S.B. Prusiner, Molecular biology of prion diseases, Science 252 (1991) 1515-1522.

[4] J.S. Griffith, Self-replication and scrapie, Nature 215 (1967) 1043-1044.

[5] C. Weissmann, Molecular genetics of transmissible spongiform encephalopathies, J. Biol. Chem. 274 (1999) 3-6.

[6] A. Aguzzi, M. Glatzel, F. Montrasio, M. Prinz, F.L. Heppner, Interventional strategies against prion diseases, Nat. Rev. Neurosci. 2 (2001) 745-749

[7] S. Hornemann, R. Glockshuber, A scrapie-like unfolding intermediate of the prion protein domain PrP(121-231) induced by acidic pH, Proc. Natl. Acad. Sci. USA 95 (1998) 6010-6014.

[8] J.W. Kelly, The environmental dependency of protein folding best explains prion and amyloid diseases, Proc. Natl. Acad. Sci. USA 95 (1998) 930-932.

[9] W. Swietnicki, M. Morillas, S.G. Chen, P. Gambetti, W.K. Surewicz, Aggregation and fibrillization of the recombinant human prion protein huPrP90-231, Biochemistry 39 (2000) 424-431.

[10] W. Swietnicki, R. Petersen, P. Gambetti, W.K. Surewicz, pH-dependent stability and conformation of the recombinant human prion protein PrP(90-231), J. Biol. Chem. 272 (1997) 27517-27520.

[11] G.S. Jackson, A.F. Hill, C. Joseph, L. Hosszu, A. Power, J.P. Waltho, A.R. Clarke, J. Collinge, Multiple folding pathways for heterologously expressed human prion protein, Biochim. Biophys. Acta. 1431 (1999) 1-13.

[12] Y. Matsunaga, D. Peretz, A. Williamson, D. Burton, I. Mehlhorn, D. Groth, F.E. Cohen, S.B. Prusiner, M.A. Baldwin, Cryptic epitopes in N-terminally truncated prion protein are exposed in the full-length molecule: dependence of conformation on pH, Proteins 44 (2001) 110-118.

[13] R. Zahn, The octapeptide repeats in mammalian prion protein constitute a pH-dependent folding and aggregation site, J. Mol. Biol. 334 (2003) 477-488.

[14] D.O. Alonso, S.J. DeArmond, F.E. Cohen, V. Daggett, Mapping the early steps in the pH-induced conformational conversion of the prion protein, Proc. Natl. Acad. Sci. USA 98 (2001) 2985-2989.

[15] D.O. Alonso, C. An, V. Daggett, Simulations of biomolecules: characterization of the early steps in the pH-induced conformational conversion of the hamster, bovine and human forms of the prion protein, Philos. Transact. A. Math. Phys. Eng. Sci. 2002 (2002) 1165-1178.

[16] L. Calzolai, R. Zahn, Influence of pH on NMR structure and stability of the human prion protein globular domain, J. Biol. Chem. 278 (2003) 35592-35596.

[17] W.L. Hubbell, H.S. Mchaourab, C. Altenbach, M.A. Lietzow, Watching proteins move

using site-directed spin labeling, Structure 4 (1996) 779-783.

[18] W.L. Hubbell, D.S. Cafiso, C. Altenbach, Identifying conformational changes with site-directed spin labeling, Nat. Struct. Biol. 7 (2000) 735-739.

[19] K.J. Oh, H. Zhan, C. Cui, K. Hideg, R.J. Collier, W.L. Hubbell, Organization of diphtheria toxin T domain in bilayers: a site-directed spin labeling study, Science 273 (1996) 810-812.

[20] L. Columbus, W.L. Hubbell, A new spin on protein dynamics, Trends Biochem. Sci. 27 (2002) 288-295.

[21] S. Mehboob, B.-H. Luo, W. Fu, M. E. Johnson, and L. W.-M. Fung, Conformational studies of the tetramerization site of human erythroid spectrin by cysteine-scanning spin-labeling EPR methods, Biochemistry 44 (2005) 15898-15905.

[22] O. Inanami, S. Hashida, D. Iizuka, M. Horiuchi, W. Hiraoka, Y. Shimoyama, H. Nakamura, F. Inagaki, M. Kuwabara, Conformational change in full-length mouse prion: a site-directed spin-labeling study, Biochem. Biophys. Res. Commun. 335 (2005) 785-792

[23] C.L. Kim, A. Umetani, T. Matsui, N. Ishiguro, M. Shinagawa, M. Horiuchi, Antigenic characterization of an abnormal isoform of prion protein using a new diverse panel of monoclonal antibodies, Virology 320 (2004) 40-51.

[24] Y. Imai, Y. Mastushima, T. Sugimura, M. Terada, A simple and rapid method for generating a deletion by PCR, Nucleic Acid Res. 19 (1991) 2785.

[25] O.H. Lowry, N.J. Rosebrough, A.L. Farr, R.J. Randall, Protein measurement with the Folin phenol reagent, J. Biol. Chem. 193 (1951) 265-275.

[26] N.R. Maiti, W.K. Surewicz, The role of disulfide bridge in the folding and stability of the recombinant human prion protein, J. Biol. Chem. 276 (2001) 2427-2431.

[27] R. Zahn, A. Liu, T. Lührs, R. Riek, C. Schroetter, F. L. García, M. Billeter, L. Calzolai, G.

Wider, K. Wüthrich, NMR solution structure of the human prion protein., Proc. Natl. Acad. Sci. USA 97 (2000) 145-150.

[28] S. Hornemann, C. Korth, B. Oesch, R. Rieka, G. Widera, K. Wüthrich, R. Glockshubera, Recombinant full-length murine prion protein, mPrP(23-231): purification and spectroscopic characterization, FEBS Lett. 413 (1997) 277-281.

[29] D. G. Donne, J. H. Viles, D. Groth, I. Mehlhorn, T. L. James, F. E. Cohen, S. B. Prusiner, P. E. Wright, H. J. Dyson, Structure of the recombinant full-length hamster prion protein PrP(29–231): The N terminus is highly flexible, Proc. Natl. Acad. Sci. USA 94 (1997) 13452-13457.

[30] R. Rick, G. Wider, M. Billeter, S. Hornemann, R. Glockshuber, K. Wüthrich, Prion protein NMR structure and familial human spongiform encephalopathies, Proc. Natl. Acad. Sci. USA 95 (1998) 11667-11672.

[31] M. Vey, S. Pilkuhn, H. Wille, R. Nixon, S.J. DeArmond, E.J. Smart, R.G. Anderson, A. Taraboulos, S.B. Prusiner, Subcellular colocalization of the cellular and scrapie prion proteins in caveolae-like membranous domains, Proc. Natl. Acad. Sci. USA 93 (1996) 14945-14949.

[32] R.J. Lee, S. Wang, P.S. Low, Measurement of endosome pH following folate receptor-mediated endocytosis, Biochim. Biophys. Acta. 1312 (1996) 237-242.

[33] G.H. Sun-Wada, Y. Wada, M. Futai, Vascuolar H^+ pumping ATPase in luminal acidic organelles and extracellular compartments: common rotational mechanism and diverse physiological roles, J. Bioenerg. Biomembr. 35 (2003) 347-358.

[34] G.H. Sun-Wada, Y. Wada, M. Futai, Lysosome and lysosome-related organelles responsible for specialized functions in higher organisms, with special emphasis on vacuolar-type proton ATPase, Cell Struct. Funct. 28 (2003) 455-63.

[35] M.L. DeMarco, V. Daggett, Local environmental effects on the structure of the prion

protein, C. R. Biol. 28 (2005) 847-862.

[36] W.-Q. Zou, N. R. Cashman, Acidic pH and detergents enhance *in vitro* conversion of human, brain PrP^{C} to a PrP^{Sc}-like form, J. Biol. Chem. 277 (2002) 43942-43947.

[37] D.A. Kocisko, S.A. Priola, G.J. Raymond, B. Chesebro, P.T. Lansbury Jr., B. Caughey, Species specificity in the cell-free conversion of prion protein to protease-resistant forms: a model for the scrapie species barrier, Proc. Natl. Acad. Sci. USA 92 (1995) 3923-3927.

[38] E. Langella, R. Improta, V. Barone, Checking the pH-induced conformational transition of prion protein by molecular dynamics simulations: effect of protonation of histidine residues, Biophys. J. 87 (2004) 3623-3632.

[39] G. E. Pake, T. L. Estle, The Physical Principles of Electron Paramagnetic Resonance, second ed., Benjamin, Inc., Reading (1973) Chapt. 6.

[40] J. Gsponer, P. Ferrara, A. Caflisch, Flexibility of the murine prion protein and its Asp178Asn mutant investigated by molecular dynamics simulations, J. Mol. Graph. Model 20 (2001) 169-182.

Legends to figures

Figure 1 A schematic diagram of the full-length moPrP and the site-directed spin labeling (SDSL) technique.

(A) The full-length moPrP and the target region for SDSL-ESR. The full-length moPrP consisted of 208 amino acids (residues 23-231). The N-terminal domain is largely flexible and has four octapeptide repeats. The C-terminal domain is comprised of three α-helices (H1, H2 and H3) and two β-sheets (S1 and S2). moPrP contains five Cu^{2+}-binding sites, two cysteines (codons 178 and 213) forming one disulfide bond, two N-glycolation sites (codons 180 and 196) and one GPI anchor (C-terminal end). The targets of cysteine mutation are seventeen amino acids at H1, S1 and S2. (B) The reaction of the methanethiosulfonate spin-labeling reagent with the cysteine residue generates the nitroxide side chain (R1) on moPrP.

Figure 2 ESR-spectra of α-helix1 (H1) mutants and effects of pH on their line shapes.

(A) ESR spectra of nine moPrP mutants at pH 7.4 (black line) and pH 5.0 (red line) were recorded using an X-band ESR spectrometer at 20°C. (B) The pH-dependent changes in domain mobility of moPrP mutants. The values of $1/\delta H$ obtained from the peak-to-peak central component ($M_I=0$) in the ESR spectra of spin-labeled $moPrP^C$ at H1 were plotted as a function of pH.

Figure 3 ESR-spectra of β-sheet1 (S1) mutants and effects of pH on their line shapes.

(A) ESR spectra of four moPrP mutants were recorded at pH 7.4 (black line) and pH 5.0 (red line) at 20°C. (B) The values of $1/\delta H_0$ of the nitroxide probes of S1 mutants are plotted as a function of pH.

Figure 4 ESR-spectra of β-sheet2 (S2) mutants and effects of pH on their line shapes. (A) ESR spectra of four S2 mutants at 20°C and pH 7.4 (black line) and pH 5.0 (red line). (B) The values of $1/\delta H_0$ of the nitroxide probes of S2 mutants are plotted as a function of pH.

Figure 5 The dependency of the mobility parameters of the ESR spectrum on the 3D structure of PrP and identification of pH-sensitive regions of PrP.

(A) The general relationship between the mobility of the nitroxide side chain and salient features of the moPrP. The inverse spectral second moments ($1/\langle H^2 \rangle$) and the inverse central linewidths ($1/\delta H_0$) for the R1 side chain at seventeen sites in moPrP are expressed as semiempirical parameters of mobility. The topographic regions of moPrP were classified into four protein folding categories; *i.e.*, the helix surface site, the helix tertiary contact site, S1 (the surface side) and S2 (the buried side). The light gray line shows the regression linear fitting between these two mobility parameters. The value, r=0.80 (n=17) of Pearson's correlation coefficient obtained from these two parameters was greater than the 1% significance value, r=0.606 (n=17), indicating that the reciprocal central linewidth was positively correlated with the inverse of the spectral second moments.

(B) The variation of mobility obtained from ESR spectra of recombinant moPrP mutants in physiological conditions (pH 7.4). Each α-carbon position indicated by graduated colors for relative mobility was superimposed on the 3D structure of moPrP as reported by an NMR study (PDB entry 1AG2, ref. 28).

(C) The 3D positions of pH-sensitive regions of PrP. The magnitude of mobility change induced by a decrease from pH 7.4 to pH 5.0 was qualitatively evaluated. Each α-carbon indicated by graduated colors for relative pH sensitivity was superimposed on the 3D structure of moPrP as reported by an NMR study [ref. 28].

Figure1

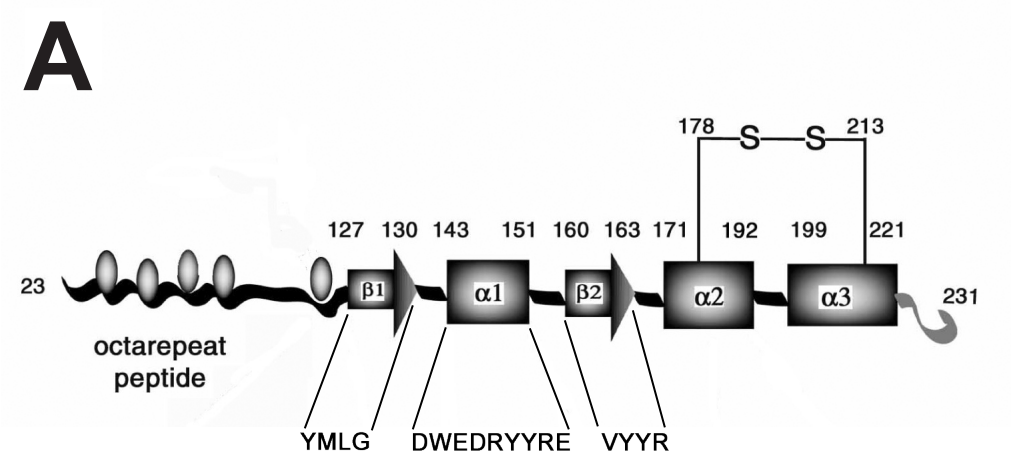

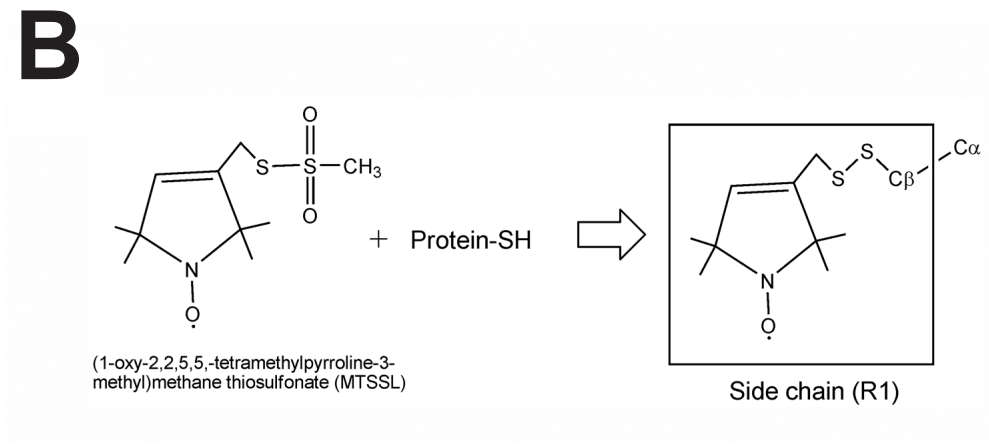

Figure 1

Figure2

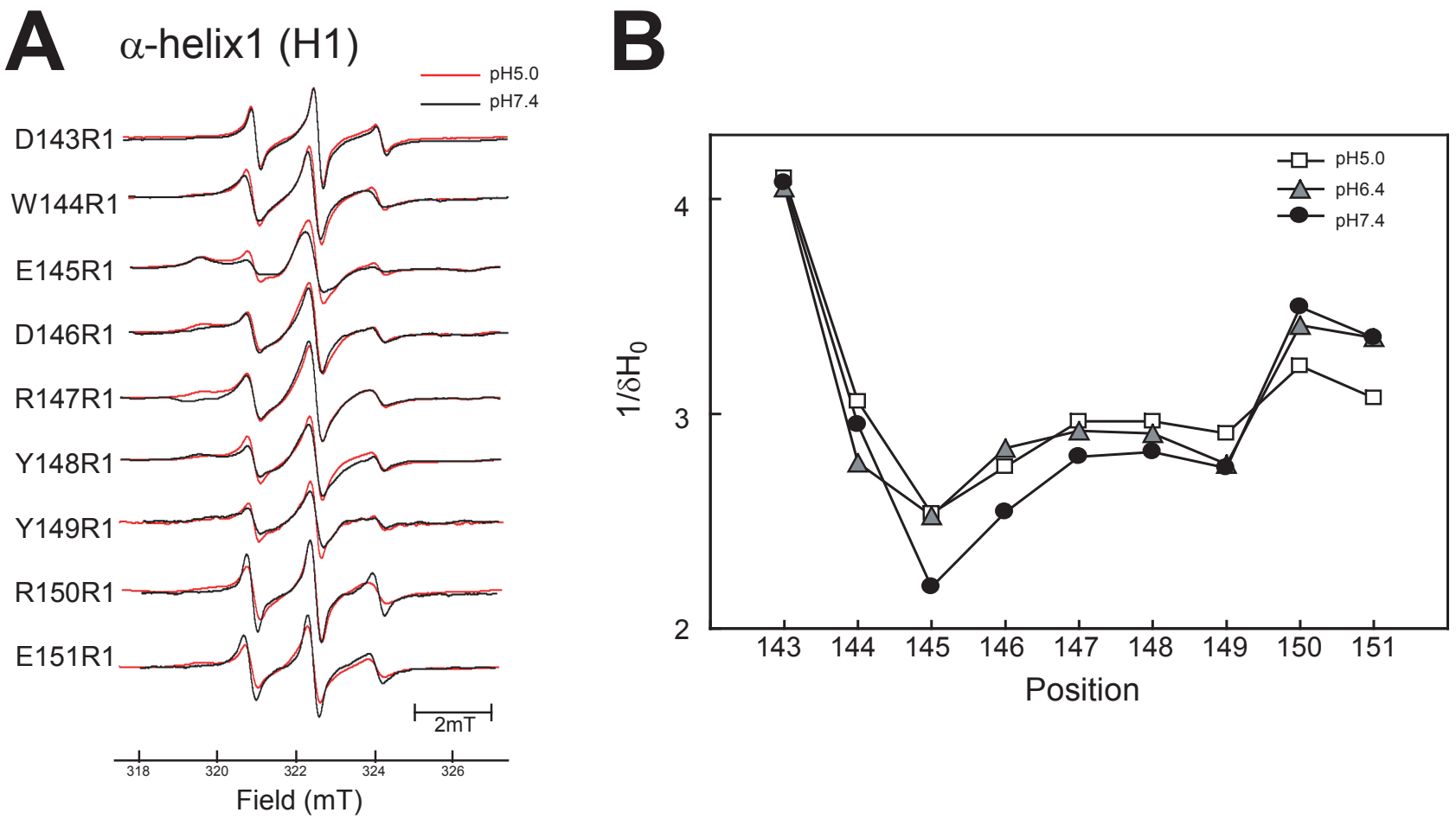

Figure 2

Figure3

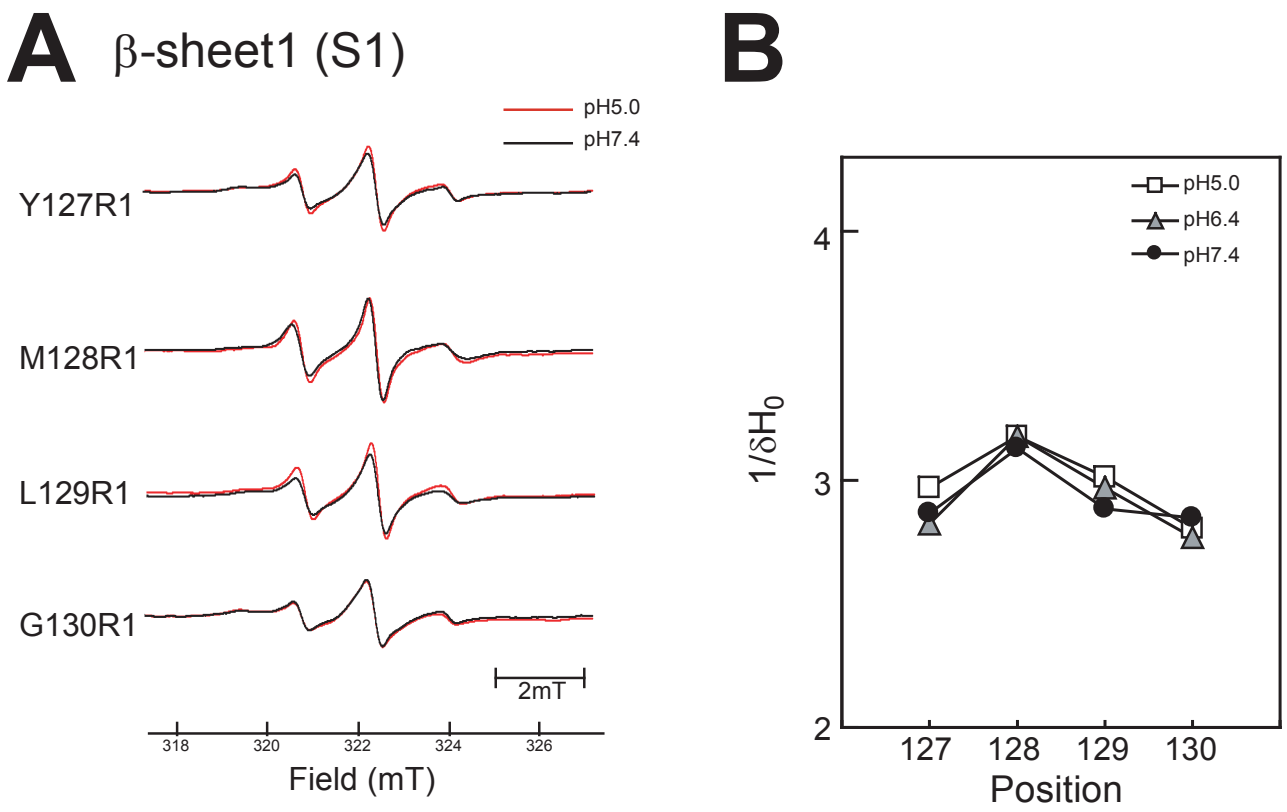

Figure 3

Figure4

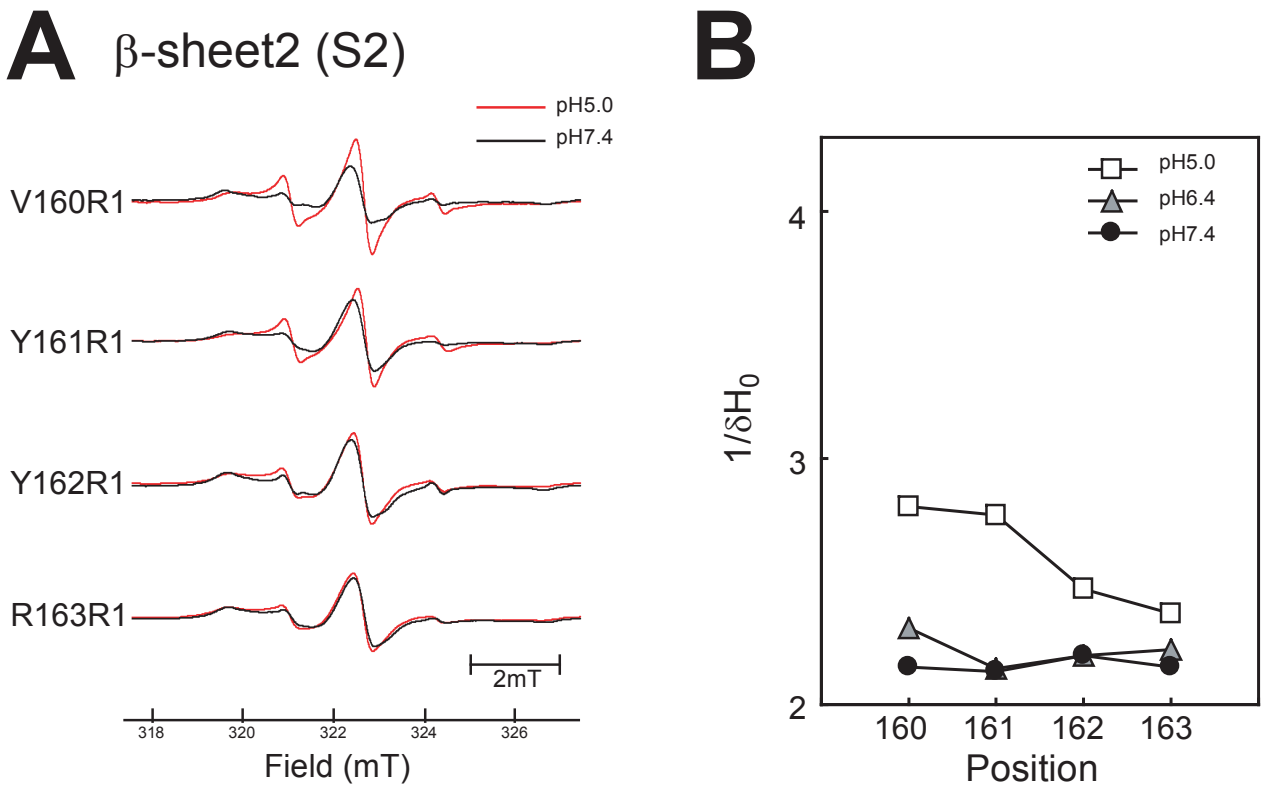

Figure 4

Figure5

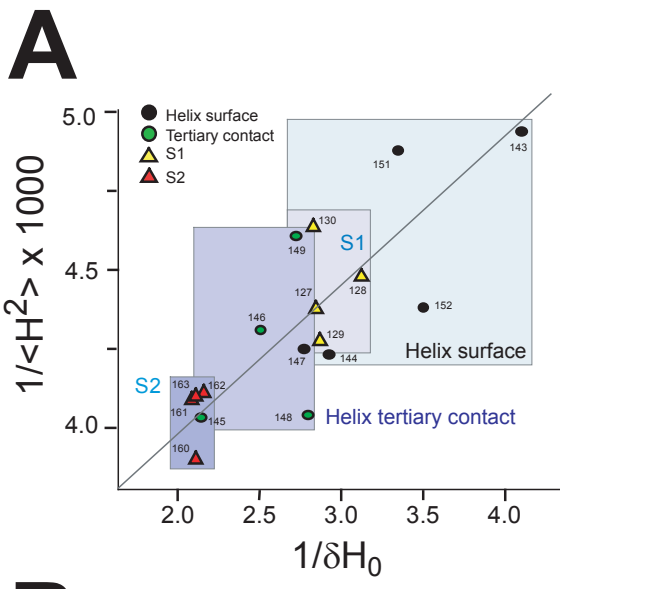

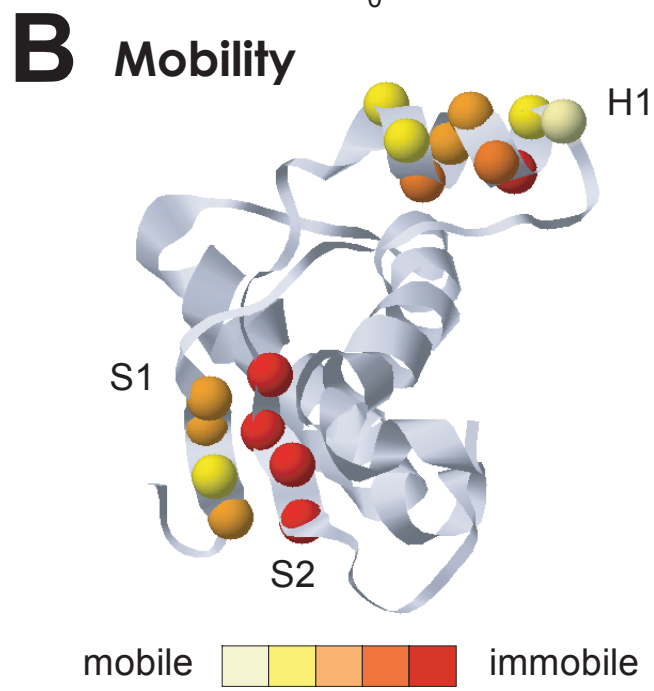

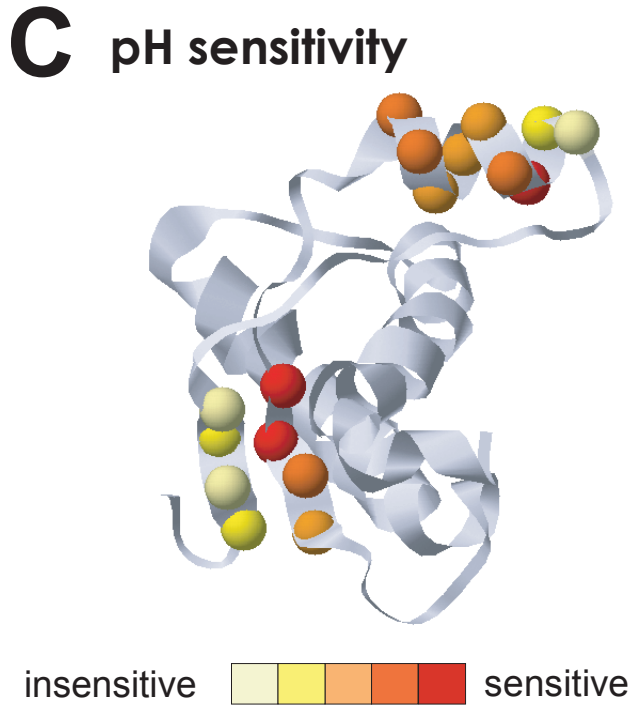

Figure 5